

Original Article

Automated three-dimensional distance and coverage mapping of hallux valgus: a case-control study

Kepler Alencar Mendes de Carvalho¹ , Andrew Behrens¹ , Vineel Mallavarapu¹ , Ryan Jasper¹ ,
Nacime Salomão Barbachan Mansur^{1,2} , Matthieu Lalevee^{1,3} , Kevin Dibbern¹ , César de César Netto¹ 

1. Department of Orthopedics and Rehabilitation, Carver College of Medicine, University of Iowa.

2. Department of Orthopedics and Traumatology, Paulista School of Medicine. Federal University of Sao Paulo.

3. Department of Orthopedic Surgery, Rouen University Hospital, Rouen, France.

Abstract

Objective: To develop distance-mapping and coverage-mapping algorithms to assess metatarsophalangeal and metatarsal-sesamoid joint interaction in hallux valgus patients, comparing them to a control group.

Methods: A total of 9 hallux valgus patients (mean age 37.1 y; 6 F/3 M) and 5 controls (mean age 39 y; 4 F/1 M) underwent weight-bearing computed tomography. Specific software was used to obtain bone segmentation images of the first and second metatarsals, the first and second proximal phalanxes, and the tibial and fibular sesamoids. Joint interaction based on distance mapping and coverage mapping of the first and second metatarsophalangeal joints and the metatarsal-sesamoid joints were calculated. The surfaces of the metatarsophalangeal joints were divided in a 2-by-2 grid using the principal axes to provide a more detailed analysis. P-values <0.05 were considered significant.

Results: Coverage maps of hallux valgus and control patients revealed marked lateral and dorsal displacement in joint interaction of the first metatarsophalangeal joint, including decreased joint coverage of the medial facet of the joint. When comparing first metatarsophalangeal joint coverage, hallux valgus patients had significantly lower coverage of the dorsomedial quadrant (77%, $p=0.0002$) than controls, as well as significantly higher coverage of the plantar lateral (182%, $p=0.005$) and dorsolateral quadrants (44.9%, $p=0.035$).

Conclusions: In this case-control study, we developed a distance and coverage map weight-bearing computed tomography algorithm to objectively assess 3D joint interaction, joint coverage, and subluxation in hallux valgus deformity. We observed significantly greater first and second metatarsophalangeal joint subluxation in hallux valgus patients than controls.

Level of Evidence III; Case Control Study.

Keywords: Imaging, three-dimensional; Hallux valgus; Metatarsal bones; Weight-bearing.

Introduction

Hallux valgus deformity (HVD) is a complex three-dimensional (3D) distortion that involves varus, dorsiflexion, and pronation of the first metatarsal. HVD is usually assessed by conventional 2D measurements, such as hallux valgus and intermetatarsal angle^(1,2). However, weight-bearing computed

tomography (WBCT) and 3D distance mapping and coverage mapping allow for assessment of the relative positioning between opposing articular surfaces. This provides information about joint coverage and joint subluxation that could influence the development of arthritic degeneration and associated symptoms, which can dictate outcomes⁽³⁾.

Study performed at the UIOWA Orthopedic Functional Imaging Research Laboratory (OFIRL).

Correspondence: Kepler Alencar Mendes de Carvalho, Department of Orthopaedic and Rehabilitation, University of Iowa, Carver College of Medicine, 200 Hawkins Dr. John PappaJohn Pavillion (JPP), Room 01066, Lower Level, Iowa City, IA, 52242, United States. **Email:** kepler-carvalho@uiowa.edu. **Conflicts of interest:** César De César Netto: CurveBeam: Paid consultant; Stock or stock Options; Foot and Ankle International: Editorial or governing board; Editor in Chief Foot and Ankle Clinics; Nextremity: Paid consultant; Ossio: Paid consultant; Paragon 28: IP royalties; Paid consultant; Weightbearing CT; International Study Group: Board or committee member; Zimmer: Paid consultant. **Nacime Salomão Barbachan Mansur:** Brazilian Foot and Ankle Society: Board or committee member; American Orthopaedic Foot and Ankle Society: Board or committee member. **Source of funding:** none. **Date received:** April 14, 2022. **Date accepted:** April 18, 2022. **Online:** April 30, 2022.



This advanced 3D imaging modality is not influenced by foot projection or orientation, allowing for visualization of multiplanar bone anatomy in an upright position. WBCT has led to significant advances, including the ability to perform traditional HVD measurements in a 3D setting that reliably and accurately assess joint morphology^(1,2,4,5). WBCT provides a more comprehensive illustration of the deformity than standard radiographs, thus allowing a better understanding of the relative positioning of the bones of the first and second rays^(1,2,4). This semi-automated technique may also reduce the potential for misinterpreting standard radiographs⁽⁶⁾.

Distance mapping, a recently developed technique for 3D analysis of the relative positions between joint surfaces (joint interaction) of the foot and ankle, provides insight into the effects of weight bearing on both healthy and pathologic conditions^(3,7-10). This 3D tool evaluates joint space in the foot and ankle across entire bony interfaces through thousands of distance measurements between opposing articular surfaces. These measurements can then be illustrated qualitatively to demonstrate the distribution of distances from the articular surface. This can be enhanced with color-coded maps for each bone, which can also be used to quantify and compare the interaction of the articular surface^(3,8-10).

The surface-to-surface interaction in a joint can be broken down into two major interrelated components. The first component consists of the contact sites and the surface pressure distribution between the hinged surfaces⁽¹¹⁻¹³⁾. The second component is the spatial relationship between joint surfaces during joint movement⁽¹¹⁻¹⁴⁾. This property can be characterized through distance maps that describe the distribution of distances between the joint surfaces at each position. In an important study, Dibbern et al.⁽³⁾ expanded upon 3D distance mapping of WBCT to assess subluxation through colored coverage mapping. These maps, which are based on distance mapping, identify areas of adequate joint interaction, joint subluxation, and impact, providing images that are more interpretable and potentially clinically useful. This facilitates

understanding of areas of interest where subluxation and impact can occur⁽³⁾.

Thus, the aim of this study was to develop a distance- and coverage-mapping algorithm to assess metatarsophalangeal (MTP) and metatarsal-sesamoid joint interactions in HVD patients and compare them to healthy controls. We hypothesized that significantly greater MTP and metatarsal-sesamoid joint lateral subluxation would be observed in the HVD group.

Methods

This retrospective case-control study was approved by the institutional review board (#202006176) and conformed to the Health Insurance Portability and Accountability Act and Declaration of Helsinki guidelines. The sample included 9 feet from patients diagnosed with HVD, which were compared to 5 feet from healthy controls, all ipsilateral.

Disior Bonelogic[®] 2.0 was used to create models of all bones proximal to the first distal phalanx in STL files. These models were then analyzed using a semiautomatic segmentation protocol in MatLab code (Mathworks Inc., Natick, MA, USA). Distance mapping was then performed to determine the boundaries of the first and second metatarsals, the proximal phalanx of the hallux, and the second toe from WBCT images. The segmentations were then reviewed by a trained doctoral researcher and exported as triangulated surface models. These models were smoothed using Geomagic Design X (Artec 3D, Luxembourg) to remove any voxelation artifacts and mild irregularities.

Distances along the entire surface of the first and second MTP joint were measured. The surfaces of the first and second MTP were divided into two-by-two grids using the principal axes of the joint surface to provide a more detailed analysis. Using the distance along the normal direction of vectors projected from the first metatarsal head subchondral surface to the opposed surface of the phalanx proximal (standard distance)^(3,14), measurements were performed in the MTP joint areas (Figures 1 and 2).

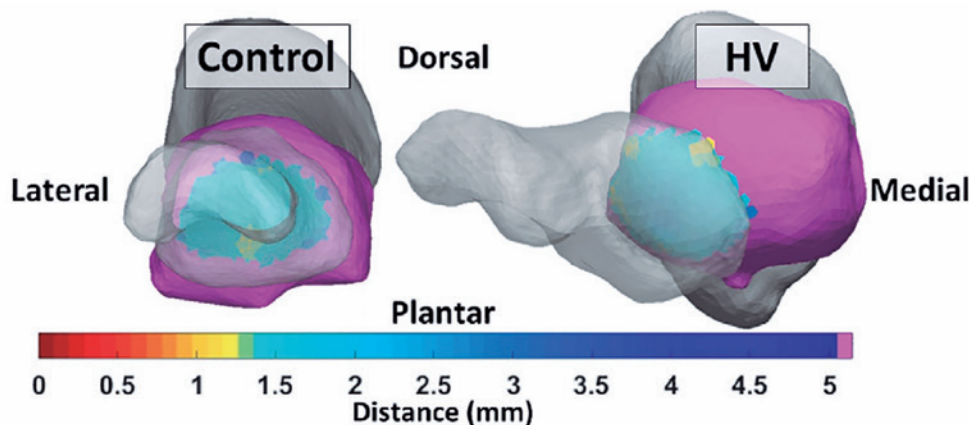


Figure 1. Summary of coverage map changes in the control (left) and hallux valgus (right) groups.

Due to the highly curved surfaces of nonarticular regions, such as the space between the first and second metatarsal bones, aberrantly large distances can exist. These distances are unrelated to loading and deviate significantly from neighboring regions⁽³⁾. To account for this, the vertical distance from each point to the opposite surface, based on the scanner's coordinate system, was used to compute distances in highly curved/uneven regions (Figure 3).

Regions of interest in distance mapping were highlighted in color (Figure 2). It has been observed that subchondral bone-to-bone distances rarely exceed 2.5 mm in the MTP joint⁽¹⁴⁾. Blue regions represent expected distances in joint interaction, which range from 1 to 3 mm. Regions > 3 mm were represented in red (Figure 2). Comparisons were performed with independent *t*-tests, assuming unequal variances, with P-values <0.05 considered significant.

Results

Figure 1 shows sample coverage maps from a HVD patient and a control, which demonstrate clear lateral and dorsal displacement of joint interaction in the first MTP joint, with decreased coverage of the medial facet of the joint. Comparison of first MTP joint coverage showed that the HVD group had significantly lower coverage of the dorsomedial quadrant (77%, $p=0.0002$), and significantly greater coverage of the plantarlateral (182%, $p=0.005$) and dorsolateral quadrants (44.9%, $p=0.035$). These findings are consistent with lateral subluxation and dorsiflexion of the first metatarsal in the first MTP joint. In the second MTP joint, the findings were consistent with the dorsiflexion contracture and dorsolateral joint subluxation characteristic of early hammertoe deformity, with significantly decreased joint coverage of the plantar-me-

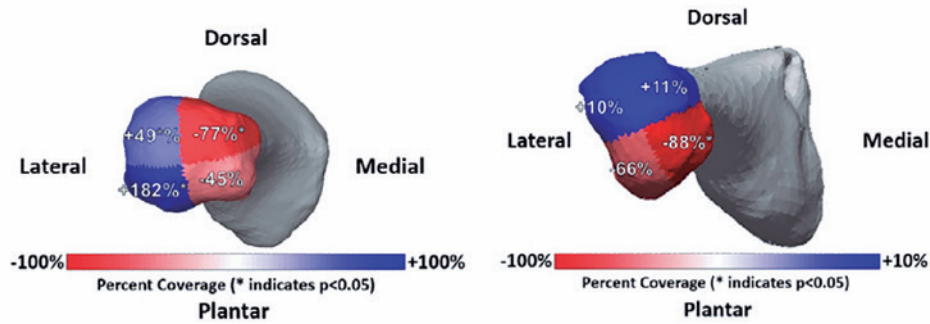


Figure 2. Summary of coverage changes in the first (left) and second (right) metatarsals.

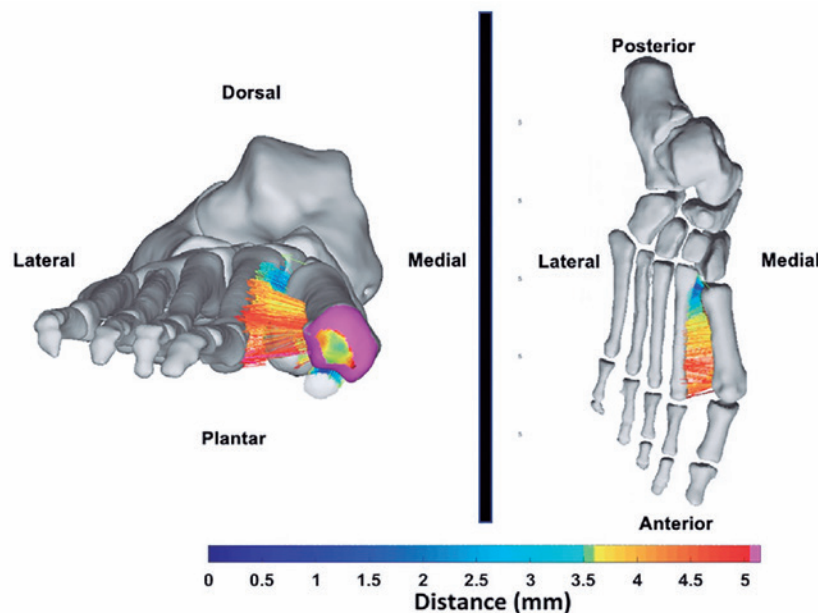


Figure 3. Average normal spacing between each point and the opposite surface in the first and second metatarsals used to calculate distances in highly curved/unequal regions.

dial quadrant (88%, $p=0.01$). Although no significant joint coverage changes were observed in the metatarsal-sesamoid joints, a significant widening of the fibular metatarsal-sesamoid joint was observed (76.7%, $p=0.013$).

Discussion

To our knowledge, this is the first study to evaluate distance and coverage maps in HVD patients, as well as the first study to use fully automated methods to compute joint coverage in the forefoot.

The normal bony anatomy of the metatarsal heads is complex due to various bony protuberances and concavities, including distinct contour changes across a spectrum of soft tissue structures. Differentiating between normal and abnormal anatomical findings can prove challenging because the typical bony structures can simulate erosive changes in the image. To better differentiate normal bone anatomy from pathologically induced changes, it is necessary to understand the normal contours of metatarsal heads⁽¹⁵⁾.

In a cadaveric study, Hull et al.⁽¹⁶⁾ attempted to determine how much of the articular surface of the MTP joint can be visualized during joint arthroscopy, finding that an average of 57.5% of the metatarsal head and 100% of the base of the proximal phalanx were visualized in distal 2D projection. They concluded that incomplete visualization of the metatarsal head occurred due to the technical limitations of their methods, demonstrating how difficult it is to visualize and properly study the articular surface of the MTP joints.

In another cadaveric study, Torshizy et al.⁽¹⁵⁾, evaluated the anatomical characteristics of the first metatarsal head with CT and MRI in an attempt to characterize contours of the metatarsal heads that can simulate erosive changes. They concluded that the normal anatomical contours of the metatarsal head may be the primary source of diagnostic error when viewing CT and MRI images in patients with suspected erosive arthritis. They also concluded that these variations, although typical, produce findings that can make distinguishing between normal and pathological states difficult.

In this context of diagnostic difficulties for 3D structures such as metatarsal heads, new technologies like WBCT and associated software for distance and coverage mapping of the forefoot can allow a better understanding of anatomical variations and the effects of weight-bearing in both healthy and pathological conditions.

This type of non-invasive methodology to quantify joint interaction was first used by Siegler et al.⁽⁹⁾ in a cadaveric study to characterize surface-to-surface interaction in the ankle and subtalar joints. They used an imaging-based distance mapping approach based on high-resolution CT, which provided detailed insight into the interaction of joint surfaces in healthy ankle and subtalar joints in neutral and extreme joint positions.

Lintz et al.⁽⁸⁾ expanded the use of distance mapping by characterizing abnormal interaction of articular surfaces in the ankle, hindfoot, and midfoot joints of cavovarus foot compa-

red to normally aligned feet. Their cavovarus group had significantly greater surface-to-surface distance at the posterior tibiotalar joint, a shorter distance at the anterior section, and a greater distance at the posterior half of the medial gutter. They concluded that distance mapping analysis of WBCT imaging could identify significant differences in surface-to-surface interaction in foot and ankle joints between cavovarus and normally aligned feet.

In a recent case-control study of stage 1 flexible progressive collapsing foot deformity patients, Dibbern et al.⁽³⁾ introduced the concept of coverage mapping images in association with WBCT and distance mapping to assess subluxation and joint impingement associated with peritalar subluxation across the entire subtalar joint surface. With this technique, they objectively identified middle facet subluxation as the only peritalar subluxation marker, with a mean 46% increase in subluxation in progressive collapsing foot deformity patients compared to controls.

Using the same technique in our study, we found significant subluxation on the medial side of the first metatarsal in HVD patients. However, beyond visualizing subluxation, which could also be done other imaging methods, we were able to quantify it for the first time in the literature. In our series, there was 77% less coverage in the upper medial facet (dorso-medial quadrant) and 45% less coverage in the inferomedial facet (medial plantar quadrant) than the control group. Similarly, inferolateral and inferomedial coverage were 66% and 88% lower, respectively, in the in the second metatarsal head.

Finally, the results of this study could have a significant impact on clinical practice. This is the first study to apply distance mapping to HVD, opening the way for future investigations of early thresholds and determining the risk of progression to HVD. Although our findings reflect known changes in HVD (subluxation of the proximal phalanx), for the first time the interaction between the joint surfaces in the MTP joints has now been quantified through distance mapping, making the assessment more objective and reproducible. The practical implications of this finding are that advanced analysis of 3D datasets with distance and coverage mapping can allow for rapid quantitative analysis of the MTP joint, rather than relying on a subjective visual assessment of the joint space.


This study has several limitations. First, the control group consisted of patients with contralateral foot and ankle injuries and deformities. Therefore, subtle asymmetries resulting from antalgic posture could confound the results. Second, no formal power analysis was performed, and our sample size may have been insufficient to demonstrate differences in some of the measurements. Third, we did not compare the findings with traditional 2D coronal plane MTP joint subluxation measurements or other classic HVD measurements. We expect a significant correlation between them, and these comparisons should be included in future investigations. Fourth, since the images were taken in a static standing position, they do not tell a dynamic story. Other parts of the gait cycle can add stress and more significant displacement of the involved topologies. In addition, we did not evaluate clinical outcomes

or correlate them with progression of HVD, thus limiting the immediate clinical implications of the findings. Future prospective and longitudinal investigations will be critical to determine the role of distance and coverage mapping in MTP joint subluxation with respect to HVD progression.

Conclusion

In this case-control study, we developed a distance- and coverage-mapping WBCT algorithm to objectively assess 3D

joint interaction and joint coverage and subluxation in HVD. We observed a significantly greater joint subluxation in HVD patients than controls in a plantar-medial and dorsolateral direction for the first and second MTP joints, respectively. No significant joint subluxation of the metatarsal-sesamoid joint was observed. Our hope is that distance and coverage mapping can optimize the diagnosis, staging, and assessment of both treatment and outcomes in HVD and lesser toe deformities. Additional appropriately sized prospective studies are needed.

Authors' contributions: Each author contributed individually and significantly to the development of this article: KAMC *(<https://orcid.org/0000-0003-1082-6490>) Conceived and planned the activities that led to the study, interpreted the results of the study, participated in the review process and approved the final version; AB *(<https://orcid.org/0000-0002-4588-9291>) Image creation, data collection and interpreted the results of the study; VM *(<https://orcid.org/0000-0002-8612-5941>) Data collection and interpreted the results of the study; RJ *(<https://orcid.org/0000-0003-3448-1300>) Data collection and interpreted the results of the study; ML *(<https://orcid.org/0000-0001-5058-8867>) Data collection and interpreted the results of the study; NSBM *(<https://orcid.org/0000-0003-1067-727X>) Interpreted the results of the study and approved the final version; KD *(<https://orcid.org/0000-0002-8061-4453>) Interpreted the results of the study and approved the final version; CCN *(<https://orcid.org/0000-0001-6037-0685>) Interpreted the results of the study and approved the final version. All authors read and approved the final manuscript. *ORCID (Open Researcher and Contributor ID) 

References

- de Cesar Netto C, Richter M. Use of Advanced Weightbearing Imaging in Evaluation of Hallux Valgus. *Foot Ankle Clin.* 2020; 25(1):31-45.
- Braza S, Mansur NSB, Mallavarapu V, Carvalho KAM, Dibbern K, Nery CAS, et al. Hallux valgus measurements using weight-bearing computed tomography: what changes?. *J Foot Ankle.* 2021;15(3):259-64.
- Dibbern KN, Li S, Vivtcharenko V, Auch E, Lintz F, Ellis SJ, et al. Three-dimensional distance and coverage maps in the assessment of peritalar subluxation in progressive collapsing foot deformity. *Foot Ankle Int.* 2021;42(6):757-67.
- Collan L, Kankare JA, Mattila K. The biomechanics of the first metatarsal bone in hallux valgus: a preliminary study utilizing a weight bearing extremity CT. *Foot Ankle Surg.* 2013;19(3):155-61.
- Welck MJ, Singh D, Cullen N, Goldberg A. Evaluation of the 1st metatarso-sesamoid joint using standing CT - The Stanmore classification. *Foot Ankle Surg.* 2018;24(4):314-9.
- Mansur NSB, Lalevee M, Schmidt E, Dibbern K, Wagner P, Wagner E, et al. Correlation between indirect radiographic parameters of first metatarsal rotation in hallux valgus and values on weight-bearing computed tomography. *Int Orthop.* 2021;45(12):3111-8.
- Day MA, Ho M, Dibbern K, Rao K, An Q, Anderson DD, et al. Correlation of 3D Joint Space Width From Weightbearing CT With Outcomes After Intra-articular Calcaneal Fracture. *Foot Ankle Int.* 2020;41(9):1106-16.
- Lintz F, Jepsen M, De Cesar Netto C, Bernasconi A, Ruiz M, Siegler S; International Weight-Bearing CT Society. Distance mapping of the foot and ankle joints using weightbearing CT: The cavovarus configuration. *Foot Ankle Surg.* 2021;27(4):412-20.
- Siegler S, Konow T, Belvedere C, Ensini A, Kulkarni R, Leardini A. Analysis of surface-to-surface distance mapping during three-dimensional motion at the ankle and subtalar joints. *J Biomech.* 2018;76:204-11.
- Bernasconi A, De Cesar Netto C, Siegler S, Jepsen M, Lintz F; International Weight-Bearing CT Society. Weightbearing CT assessment of foot and ankle joints in Pes Planovalgus using distance mapping. *Foot Ankle Surg.* 2021:S1268-7731(21)00205-8.
- Kimizuka M, Kurosawa H, Fukubayashi T. Load-bearing pattern of the ankle joint. Contact area and pressure distribution. *Arch Orthop Trauma Surg.* 1980;96(1):45-9.
- Calhoun JH, Li F, Ledbetter BR, Viegas SF. A comprehensive study of pressure distribution in the ankle joint with inversion and eversion. *Foot Ankle Int.* 1994;15(3):125-33.
- Corazza F, Stagni R, Castelli VP, Leardini A. Articular contact at the tibiotalar joint in passive flexion. *J Biomech.* 2005;38(6):1205-12.
- Moeller T. Normal findings in radiography. Translation of the 2nd, German ed. New York: Thieme; 2000.
- Torshizy H, Hughes TH, Trudell D, Resnick D. Anatomic features of metatarsal heads that simulate erosive disease: cadaveric study using CT, radiography, and dissection with special emphasis on cross-sectional characterization of osseous anatomy. *AJR Am J Roentgenol.* 2008;190(3):W175-81.
- Hull M, Campbell JT, Jeng CL, Henn RF, Cerrato RA. Measuring visualized joint surface in hallux metatarsophalangeal arthroscopy. *Foot Ankle Int.* 2018;39(8):978-83.